RSC Advances

ROYAL SOCIETY OF CHEMISTRY

www.rsc.org/advances

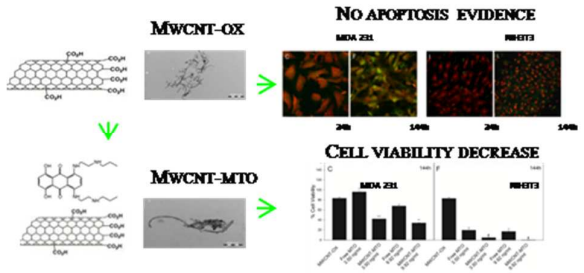

Cite this: DOI: 10.1039/c0xx00000x

www.rsc.org/xxxxxx

ARTICLE TYPE

In vitro study of Multiwall Carbon Nanotubes (MWCNTs) with adsorbed Mitoxantrone (MTO) as a drug delivery system to treat breast cancer.

Giulia Risi[1], Nora Bloise[2], Daniele Merli[1], Antonia Icaro-Cornaglia[3], Antonella Profumo[1], Maurizio Fagnoni[1], Eliana Quartarone[1] Marcello Imbriani[3,4], Livia Visai[2,4].

Received (in XXX, XXX) Xth XXXXXXXXX 20XX, Accepted Xth XXXXXXXXX 20XX
DOI: 10.1039/b000000x

Abstract:

Mitoxantrone (MTO) is a well-known anticancer drug. In order to improve its therapeutic effect, multi-walled carbon nanotubes (MWCNTs) were studied *in vitro* as a drug delivery system. We performed a comparative analysis of the *in vitro* cytotoxicity, internalization and MTO loading capacity of MWCNTs in: i) MDA 231, a breast cancer cell line, and ii)NIH3T3, a non-neoplastic fibroblast cell line. MWCNT cytotoxicity was time- and dose-dependent for MDA 231, whereas NIH3T3 survived longer incubation times. A MWCNT dose of 0.4 μg/mL free of cytotoxic effects was chosen for further experiments. MWCNTs internalization was evidenced by TEM. MTO release from MWCNTs showed linear kinetics over a 24 h period. For both cell types, MWCNT-MTO cytotoxic effects were time- and dose-dependent, and greatly improved with respect to the soluble drug at long incubation times. MTO delivery through MWCNTs is efficient in both cell types, without distinctions between cancer and non-neoplastic cells.

1.0. Introduction

Targeted drug delivery using suitable vectors is considered a valuable strategy to administer drugs and is aimed at improving their therapeutic effect, and at the same time reducing systemic toxicity. This approach is parallel to the development of new therapeutic agents with higher selectivity and better pharmacological profile[1]. In this regard, due to the severity of some neoplastic illnesses with poor prognosis, the use of nanovectors with some intrinsic toxicity and possible long-term harmful effects is acceptable if an immediate benefit is clearly shown[2].

Carbon nanotubes (CNTs), because of their stability, inertness, and higher surface area-to-volume ratio (as compared with spheres) are considered a good candidate as a nanovector. Furthermore, CNTs are gaining more and more interest because of their easy surface functionalization and their ability to cross cell membranes[3]. The application of carbon nanotubes in drug delivery systems was immediately conceptionalized after the first demonstration of their capacity to penetrate into cells[4]. Several *in vitro* studies have demonstrated that carbon nanotubes can effectively transport various molecules including drugs, peptides, and proteins into cells[5-10]. However, contradictory results on CNTs toxicity have been reported[11], thus in depth studies on their cytotoxicity are necessary. To the best of our knowledge, the influence of CNTs on important cellular physiological processes, such as cell adhesion and migration, have not yet been well documented[12].

CNTs are classified as multi-walled (MWCNTs) or single-walled (SWCNTs) moieties[13]. Due to their high hydrophobicity, low functionality and large size, carbon nanotubes must be modified through covalent or non-covalent functionalization of their external walls to allow a wider biological application. CNTs are widely used for *in vitro* and *in vivo* studies for cancer therapy[14]. Ali-Boucetta *et al.* investigated the ability of the anticancer drug doxorubicin (DOX) to interact non-covalently with non-functionalized MWCNTs at various mass ratios, and evaluated their capacity to kill human breast cancer cells[15]. They demonstrated the formation of a complex and the increased cytotoxic activity of DOX loaded on MWCNTs as compared to free DOX. Sobhani *et al.* first functionalized MWCNTs using hyper branched polycitric acid (PCA), which they then conjugated to the antineoplastic drug, paclitaxel (PTX) at the carboxyl functional groups of PCA via a cleavable ester bond, to obtain a MWCNT-PCA-PTX conjugate[16]. *In vitro* cytotoxicity studies, performed on A549 and SKOV3 cell lines, revealed that MWCNT-PCA-PTX was more cytotoxic than the free drug. Samorì *et al.* conjugated MWCNTs with methotrexate (MTX) using a variety of cleavable linkers, and demonstrated that the cytotoxic efficacy of the conjugates was dependent on the type of cleavable linker used[17]. Wu *et al.* developed a MWCNT-based drug delivery system by covalently combining MWCNTs with the antineoplastic 10-hydroxycamptothecin (HCPT) drug, using hydrophilic diaminotriethylene glycol as a spacer, and demonstrated that the conjugates were superior in activity to clinical HCPT formulation both *in vitro* and *in vivo*[18]. Wu *et al.* used PEG-functionalized MWCNTs (also studied by Ravelli *et al.*[19]) as a drug delivery vehicle for the anticancer drug oxaliplatin[20]. For a detailed review on CNT PEGylation see Ravelli *et al.*[21]. It was found that PEGylation of MWCNTs was able to retard the release rate of oxaliplatin, thus improving the pharmaceutical action of the drug in HT-29 cells.

Among the different chemotherapeutic agents that can be loaded on CNTs, we focused our study on mitoxantrone (MTO). MTO is a cytotoxic member of the anthracenedione family, which acts by

intercalating with DNA and inhibiting topoisomerase II enzyme activity, involved in DNA repair[22,23]. Due to its immunosuppressive properties, it reduces B cells number, inhibits T helper cell function and augments T cell suppressor activity. MTO is widely used for the treatment of breast cancer and leukemia, and to date it has been approved in 50 different countries for the treatment of other malignancies such as hepatoma and non-Hodgkin lymphoma[24]. Well-known side effects of MTO include cardiotoxicity, seen in patients treated with high cumulative doses, a persistent decrease in circulating white blood cells and platelets and, in female patients, transitory or persistent amenorrhoea[24]. However, this drug shows considerably less acute side-effects (including nausea, vomiting, alopecia) than other chemotherapy agents[25]. MTO treatment should be established only after a careful assessment of the individual patients' risk and benefit profiles. Moreover, MTO-treated patients need to be followed-up after the end of treatment to control the risk of serious long term adverse events.

In view of these considerations, we investigated the effectiveness (in terms of cytotoxicity) of MWCNT–MTO supramolecular complex, by optimizing the binding strategy and the activity of the resulting product on a breast cancer cell line (MDA 231) in comparison with that of free MTO. Because of the lack of studies on the interaction of CNT-based drug delivery systems in non-neoplastic cell lines, we also report data from a comparative study in a fibroblast cell line (NIH3T3).

2.0. Materials and Methods

2.1. Preparation of materials and chemical characterizations

2.1.1. Purification and functionalization of MWCNTs

The presence of metallic impurities on CNTs could dramatically change their biological action, thus a purification step before CNTs use is mandatory. For this reason, MWCNTs were refluxed in hydrochloric acid following a known procedure to eliminate metallic impurities[26]. Briefly, 1 g of as-received MWCNTs were sonicated with 20 ml 20 % HCl and refluxed for 4 h .The resulting MWCNTs were separated by centrifugation at 4500 rpm for 10 min, washed with 50 ml water and centrifuged at 4500 rpm for 10 min; this last procedure was repeated 3 times, until the water layer is neutral.

An oxidation step was then performed to introduce carboxylic acid functionality on the MWCNT surface (MWCNT-OX) as previously reported[27,28].The MWCNTs (500 mg) were refluxed in a mixture (25 mL) of concentrated H_2SO_4/HNO_3 (3:1, v/v). The resulting suspension was then diluted with icy water (50 mL). Excess inorganic acid and water were removed by centrifugation (see before). The black solid obtained was treated with 10 ml 0.1 M NaOH and then with 10 ml 0.1 M HCl to remove oxidation debris, and then with distilled water (10 ml) until the eluates were neutral, centrifuging after each treatment. The MWCNT–OX obtained were dried under vacuum at room temperature. TGA analysis showed a 8 % loss at 400-600° C, which correspond to a functionalization of 1 COOH every 45 C atoms, as previously reported[26].

As CNTs tends to form aggregates of same μm diameters in a reversible manner, they can be easily separated by centrifugation or filtration. As reported below (section 3.2), one major goal was to find a dispersion procedure able to disperse these aggregates, reducing them in the nm range, as shown by TEM.

2.1.2. Mitoxatrone adsorption on MWCNT-OX

Three strategies for binding MTO to MWCNT-OX were tested: covalent attachment with (by 1-ethyl-3-(3-dimethylaminopropyl) carbodiimide, EDC (a) or dicyclohexylcarbodiimide, DCC (b) and non-covalent attachment (c). In the first two cases, the approach involved the formation of an amide bond between the carboxylic group of MWCNT-OX and the amine groups on MTO thus recurring to a carbodiimide as a condensing agent (EDC or DCC).

a) Covalent coupling mediated by EDC[29]. 25 mg of MWCNT-OX were suspended in 5 mL of 25 mM phosphate buffer (pH, 7) and sonicated for 20 min; 2 mL of a solution containing 400 mM EDC + 100 mM, NHIS in 25 mM pH, 6 MES buffer were then added. The suspension was further sonicated for 15 min, centrifuged at 3000 rpm for 5 min and the supernatant was eliminated. At this point, 2.5 mL of an opportune amount of MTO water solution (1 mg/mL in a typical experiment, to which data in Tab 1 are referred) were added. The suspension was stirred overnight in the dark, centrifuged at 4500 rpm and then analysed spectrophotometrically to establish the amount of unbound drug. The resulting MWCNT-OX complexes (EDC-MWCNT-MTO) were washed with 50 mL water and dried at 40° C for 12 h. The obtained powder (15 mg) was sealed in a glass vial.

b) Covalent coupling mediated by DCC[30]. Anhydrous conditions (including glassware) were required for this procedure. 25 mg of MWCNT-OX were suspended in 2.5 mL anhydrous dimethylformamide (DMF); 1 mg4-dimethylaminopyridine (DMAP) were added and the suspension was stirred for 10 min. The opportune quantity of MTO dissolved in 2.5 ml DMF (1 mg/ml in a typical experiment, to which data in Tab 1 are referred) were added to the MWCNT-OX suspension. The mixture was stirred overnight, centrifuged at 4500 rpm, washed with DMF (10 mL) and ethanol (20 mL) and treated as in the previous case. We obtained a 22 mg powder of DCC-MWCNT-MTO.

c) Non-covalent coupling. As carboxylic groups on MWCNT-OX and amine groups on MTO may form ammonium salts, a non-covalent strategy was investigated. Briefly, 25 mg MWCNT-OX were suspended in 2.5 mL of MTO solution (concentration range between 0.5 and 3 mg/mL H_2O) and sonicated for 5 min. The suspension was kept in the dark overnight, centrifuged at 4500 rpm, washed with water (10 mL), and treated as described in a), yielding 25 mg of MWCNT-MTO.

In addition, tests were performed to immobilize MTO onto pristine MWCNT by π-π stacking of the MWCNT surface and the anthracene ring of MTO (the same protocol as described for MWCNT-OX), to obtain pristine-MWCNT-MTO.

2.1.3. Physico/Chemical Characterization

Classical analytical techniques, and namely Thermo Gravimetric Analysis (TGA) (a), Raman spectra (b) and Transmission Electron Microscopy (TEM) images (c) to characterize the previously obtained materials were used.

a) TGA analysis. TGA (TA Instruments 2910) measurements were performed in a temperature range of 30 to 800° C, with N_2 purge. The heating rate was 5° C/min[26].

b) Raman Spectra. Micro-Raman spectroscopy measurements were carried out using a LabramDilor Raman H10 spectrometer equipped with an Olympus HS BX40 objective and with a cooled CCD camera as a photo-detector. The 632.8 nm (1.96 eV) light from a He–Ne laser was used as excitation radiation, with a total power of about 7 mW. A 100× objective was used, with spatial resolution slightly less than 1 μm. The power density incident on the sample was ~1 $\mu W/\mu m^2$ so that heating effects could be excluded. A grating with 1800 grooves/mm was used. The sample was mounted on the motorized x–y stage of the microscope, and all measurements were made at room temperature and normal pressure. The typical integration time was 60 s. The parameters of the Raman modes were best-fitted using Lorentzian curves as the fitting function[26].

c) TEM analysis. TEM analysis was performed by using a JEOL JEM 3010 operating at a 300 kV acceleration voltage. Pristine MWCNTs, MWCNT-OX and MWCNT-MTO were dispersed in water (concentration of 1 mg/mL), sonicated and deposited on Parlodion™ membranes.

2.1.4. Mitoxantrone stability and kinetic release from both covalently and non covalently MTO bound to MWCNT-OX

The chemical stability of MTO in water, biological buffer and in culture medium was assayed to confirm that during the biological experiments (up to 144 h) degradation of the drugs did not occurred. Stability was evaluated at 20 and 37° C, in non-deoxygenated culture medium and Petri dishes, which were not light-protected, respectively. The MTO concentration tested ranged from 0.1 to 6 mg/L and these were analysed by HPLC[31] at different times (3 h, 24 h, 72 h and 144 h).

For the study of *in vitro* release of MTO from the adducts of MWCNT-MTO (adsorbed, see Table 1), 1 mg/ml suspensions in Leibovitz's culture medium were prepared, sonicated (5 min, 25° C) stirred for different times (1 h, 3h, 6h, 24 h, 72 h, 144 h), centrifuged and supernatants analysed in HPLC[31].

2.1.5. Sterilization procedures

Carbon nanotubes were sterilized by gamma radiation according to a published procedure[26].

2.2. Biological characterizations

2.2.1. Cell culture conditions

The human breast cancer cell line, MDA 231 (HTB26)[32] as well as the murine fibroblast cell line, NIH3T3 (CRL1658) were obtained from the American Type Culture Collection (ATCC, Manassas, VA, USA). MDA 231 cells were cultured in Leibowitz's medium (Invitrogen) supplemented with 10 % Fetal Bovine Serum (Biowest), 0.5 % antibiotics (penicillin and streptomycin, Lonza), and 0.2 % Fungizone™ (Euroclone). NIH3T3 cells were cultured in DMEM modified medium with 4.5 g/L glucose (Invitrogen), supplemented with 10 % Bovine Calf Serum (Sigma Aldrich) and 1 % L-glutamine (Lonza). Both cell lines were incubated at 37° C with 5 % CO_2, routinely trypsinized after confluence, counted, and seeded into wells.

2.2.2. MWCNT-OX and MWCNT-MTO Dispersibility by Scanning Electron Microscopy (SEM)

To evaluate their dispersibility[33], MWCNT-OX (concentration of 1 mg/ml) or MWCNT-MTO (loading 0.25 mg MTO/g MWCNT) were dispersed in sterile 0.5 % BSA (Sigma Aldrich), 1 % DMSO (Sigma Aldrich), or in cell culture medium and then incubated with or without both cell types seeded on sterile Thermanox plastic coverlips (NalgeNunc International, Rochester, NY, USA) placed at the bottom of 24-well tissue culture plates for 24 and 144 h. At the end of each incubation time, the samples were fixed with 2.5 % (v/v) glutaraldehyde solution in 0.1 M Na-cacodylate buffer (pH, 7.2) for 1 h at 4° C, washed with Na-cacodylate buffer, and then dehydrated at room temperature in a gradient ethanol series up to 96 %. The samples were kept in 96 % ethanol for 15 min, and then critical point dried with CO_2. The specimens were sputter-coated with gold and observed with a Leica Cambridge Stereoscan 440 microscope (Leica Microsystems, Bensheim, Germany) operating at 15 kV and a magnification of 200x[34]. Furthermore, the degree of macrodispersion of both MWCNT-OX and MWCNT-MTO was then measured as previously reported[33] (data not shown).

2.2.3. Cell viability assay

Cell viability was assayed with the dye exclusion test using a 0.4 % Trypan Blue Solution (Sigma Aldrich)[35]. MDA 231 or NIH3T3 cells in the exponential growth phase were seeded on 96-well plates at a density of 1×10^4 viable cells/well. After 4 h incubation (the time to allow cell attachment to the wells), two different experiments were performed:

a) Both cell types were cultured with different concentrations (from 0.4 to 3 μg/ml) of MWCNT-OX (dispersed in 0.5 % BSA), and incubated at 3 different times (24 h, 72 h and 144 h). The concentration of MWCNT-OX that resulted as non-cytotoxic was used in further experiments with MWCNT-OX adsorbed with MTO.

b) Both cell types were cultured with different concentrations of sterile MTO (from 3.50 to 27.3 ng/ml) adsorbed on 0.4 μg/ml MWCNT-MTO or with the same amount of free MTO for 24 h, 72 h and 144 h.

At the end of each incubation time, to measure cell viability percentage, the cells from all test groups were harvested by trypsinization using a 0.05 % trypsin–EDTA solution and viable cells were then determined by Trypan blue dye exclusion using a Vi-CELL™ XR Cell Viability Analyzer (Beckman Coulter, USA).

In all viability assays, cell treatments were performed in triplicate and the results of three independent experiments were reported (n = 3).

2.2.4. Annexin V Staining

Apoptosis plays an important role in tissue homeostasis. The annexin V technique detects apoptosis by targeting the loss of phospholipid asymmetry in the plasma membrane. The loss of plasma membrane asymmetry is an early event in apoptosis, independent of cell type, resulting in the exposure of phosphatidylserine (PS) residues at the outer plasma membrane leaflet[36].

To determine apoptosis, both cell types were labeled using the PSVue480™ cell stain according to the manufacturer's instructions (Molecular Targeting Technologies, Inc.). Briefly, MDA 231 or NIH3T3 cells were seeded on glass coverlips (Thermo Scientific) at a density of 1 x 10^5 cells per well and incubated with H_2O_2 (positive control; 100 mM for 18 h), without MWCNT-OX (negative control), and with 0.4 μg/ml of MWCNT-OX for 24 h and 144 h respectively. At the end of each culture condition, cells were stained with PSVue480™ solution prepared as follows: a 2 mM solution of pre-weighed apo-

PSS480 was prepared in DMSO until the solid apo-PSS480 was fully dissolved; an equal volume of 4.2 mM zinc nitrate solution was then added. The resulting solution was placed in a water bath at 37° C and shaken frequently for 30 min to ensure complete complex formation. A clear orange solution of 1 mM stock PSVue480™ in 1:1 DMSO/water resulted. The samples were stained with 10 µM PSVue480™ by gently shaking for 2 h at room temperature and finally washed with TES buffer, composed of 5 mM TES (n-[tris(hydroxymethyl]-2-aminoethanesulfonic acid, Sigma Aldrich) and 145 mM NaCl in distilled water. Samples were then counterstained with a propidium iodide solution (2 µg/mL) to target the cellular nuclei, and observed with a Confocal Laser Scanning Microscope (CLSM) (Leica TCS SPII Microsystems, Bensheim, Germany) at 63x magnification[37].

2.2.5. Assessment of MWCNT-OX and MWCNT-MTO uptake by Transmission Electron Microscopy (TEM)

In order to establish MWCNT-OX and MWCNT-MTO cell uptake, both cell types were seeded at a density of 1×10^5 viable cells/well at the bottom of a 24-well tissue culture plate and allowed to attach to the wells for 4 h. Then, samples were exposed or not to 0.4 µg/ml MWCNT-OX and MWCNT-MTO for 3 h, 24 h and 144 h, respectively. At the end of the incubation times, cells were washed in PBS, and then fixed in Karnovsky's fixative containing 2 % paraformaldehyde, 2.5 % glutaraldehyde in 0.1 M cacodylate buffer (pH, 7.4) at 4° C for 4 h. The samples were washed with 0.1 M sodiumcacodylate buffer (pH, 7.4), post-fixed in 1 % osmium tetraoxide in collidine buffer for 1 h at 4°C, and then dehydrated via an ice-cold EtOH gradient series (25 %, 50 %, 75 %, 80 %, 90 % and 100 %) for 15 min each. The cells were covered with an ultrafine epoxidic film (Fluka) and incubated overnight at 60° C to polymerize the resin. The solid film with embedded cells was mechanically scraped and the Epon™ sheet is then observed by light microscopy. Preselected areas of the sheet were re-included in silicon molds and ultrathin sections of 75-90 nm of thickness were placed on nickel grids. Finally, grids were stained with a saturated solution of uranyl acetate followed by Reynold's lead citrate, then the stained grids were examined under a Jeol Transmission Electron Microscope (TEM)[38].

2.3. Statistical analysis

Each experiment consisted of three replicates for each condition and each was repeated three times. Results are expressed as the mean ± standard deviation. In order to compare the results between the control sample and each treated sample, the t-test analysis was applied ($p<0.05$).

3.0. Results

3.1. Physico-chemical characterization of MWCNT-OX and MWCNT-MTO

Different features of the obtained complexes were compared, namely the ease of preparation, amount of drug present on MWCNTs, release of the drug in a reasonable amount of time (hours and not minutes), and cytotoxicity[39]. Table 1 shows the amount of MTO linked to the different MWCNTs as a function of the immobilization protocol (evaluated by HPLC analysis of the supernatant). The MWCNTs were treated with a 1 mg/mL MTO solution in water or DMF as described in 3.1.2.As reported in Table 1, the amount of MTO bound to DCC-MWCNT-MTO was twofold with respect to the amount bound to EDC-MWCNT-MTO, so the EDC-based protocol was not utilized further. Analogously, the amount bound to EDC-MWCNT-MTO is similar to the amount bound to pristine-MWCNT-MTO based on the π-π stacking of the MWCNT surface and the anthracene ring of MTO. In the last two cases, the amount of MTO that could be loaded did not change with increasing concentrations of MTO in the solution. In contrast, in the case of DCC or the electrostatic protocol, the amount of MTO that could be loaded changed with the concentration of MTO in the solution, indicating greater flexibility in the loading procedure. Taking into consideration the *in vitro* results of DCC-MWCNT-MTO and MWCNT-MTO, the ease and the low cost of preparation, the non-covalent immobilization procedure is preferable.

Table 1: HPLC results (in terms of mg MTO/g MWCNTs ratio) of MTO loading on different preparations of MTO-MWCNTs complexes.Standard deviations are reported.

Sample	mg MTO/g MWCNTs
EDC-MWCNT-MTO	42 ± 3.5
DCC-MWCNT-MTO	98 ± 7.1
MWCNT-MTO (adsorbed)	97 ± 5.0
pristine-MWCNT-MTO	41 ± 3.3

By putting into contact different concentration of MTO (always 5 mL solution)with MWCNT-OX (always 50 mg), it is possible to obtain different loading contents, whose biological activity was individually tested. (Figure 1)

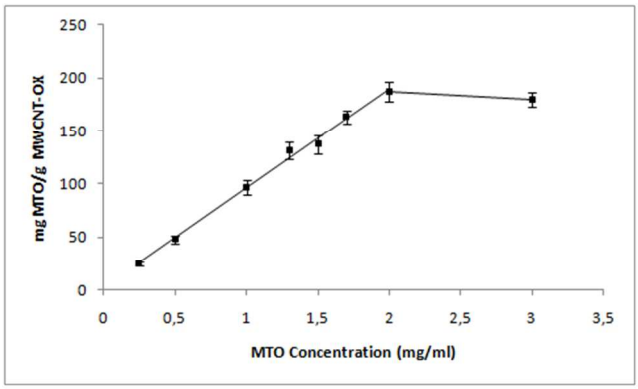

Figure 1. Loading results: ratio of different concentrations (mg/ml) of MTO adsorbed on MWCNT-OX. Standard deviations are reported.

As reported in Figure 1, when the concentration of MTO in solution reached 2 mg/mL, a plateau in the adsorption occurred, indicating that saturation of the adsorption sites was reached. In detail, when the concentration of MTO in solution is < 2 mg/mL, the adsorption behaviour is linear and can be described by the regression line: loading (mg MTO/g MWCNT-OX) = 95.244* MTO concentration (mg/mL) ($R^2 = 0.992$).

The amount of MTO immobilized onto the MWCNT-OX surface was deduced by quantifying, by HPLC, the amount of MTO still present in the solution. The results were confirmed by direct TGA analysis of MTO and MWCNT-OX adducts, and in all cases

differences of less than 10 % between the two methods of analysis were found. The MTO adducts (EDC-MWCNT-MTO, DCC-MWCNT-MTO, MWCNT-MTO) were also characterized by Raman and TEM analyses, on 20 mg MTO/ g MWCNT-MTO samples.

The comparison of Raman spectra obtained with, MWCNT-MTO, free MTO and pristine MWCNTs showed, in the case of derivatized MWCNTs, that the ratio of the D band centered at 1330 cm^{-1} and the G band centered at 1660 cm^{-1} increased as expected; an effect of the major surface disorder introduced by the functionalization[40,41] (Figure 2).

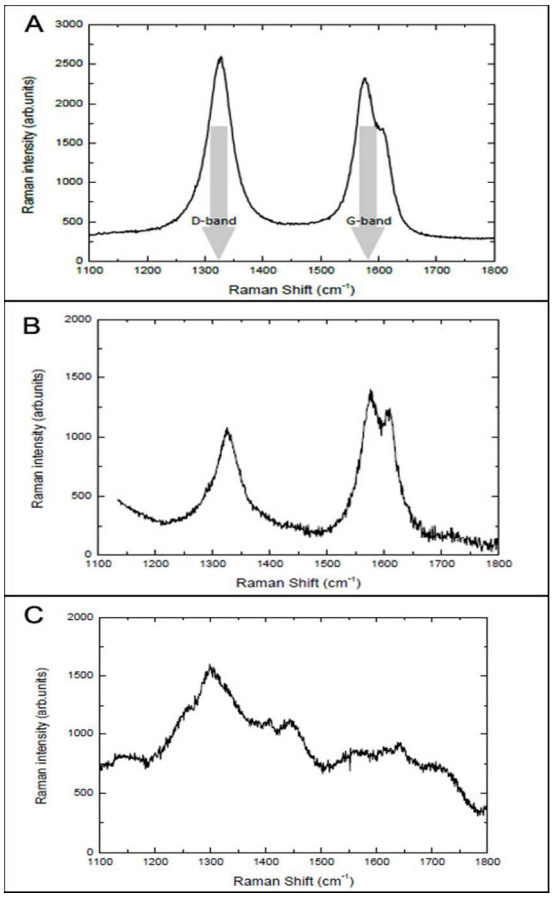

Figure 2. Raman spectra in the region of G and D modes of purified MWCNT (panel A), MWCNT-MTO loading 20 mg/g MWCNT-MTO (panel B) and MTO (panel C).

Moreover, a G' band at 1615 cm^{-1} appears, as confirmation of the alteration of the MWCNT structure. The line-widths associated with MTO-derivatized MWCNTs (both classes) are larger with respect to pristine MWCNTs, as further confirmation of the derivatization due to the MTO grafting to the surface. The characteristic vibrational modes of MTO are not appreciable in the adducts, as MTO has two characteristic bands centered at 1300 cm^{-1} and 1600 cm^{-1}, thus superimposing the MWCNT bands.

The morphology of pristine MWCNTs, MWCNT-OX and MWCNT-MTO was observed by TEM (Figure 3).

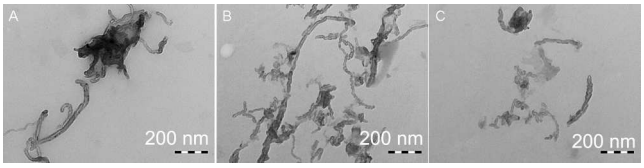

Figure 3. TEM images of pristine MWCNTs (panel A), MWCNT-OX (panel B) and MWCNT-MTO loading 20 mg/g MWCNT-MTO (panel C). Scale bar 200nm.

TEM images of pristine MWCNTs (panel A) showed that pristine materials were present as highly electron-dense bundles, whereas both the derivatized MWCNTs were less electron-dense due to the interruption on the electron dislocation of the π MWCNTs' system caused by the introduction of carboxylic groups. The MWCNT-OX were also well separated, due to the electrostatic repulsion between the charged groups; in Figure 3 (panel B) these characteristics, as well the internal structure of the MWCNTs, are evident. Panel C shows the non-covalent addition of MTO does not change the situation dramatically (we acquired many images of different sample sections, with the same results).

3.2. Evaluation of MWCNT-OX and MWCNT-MTO dispersibility

MWCNT-OX or MWCNT-MTO complexes (at 0.4 µg/mL) were dispersed in culture medium or in sterile 0.5 % BSA and incubated for 24 h and 144 h at 37° C alone (data not shown) or added to MDA 231 cells seeded in tissue culture plates. At the end of the incubation, samples were prepared for SEM observation (Figure 4a and b). SEM images are representative of both dispersed (0.5 % BSA) and non-dispersed MWCNT-OX or MWCNT-MTO complexes (in culture medium), highlighting the size and the amount of the formed aggregates.

The most important difference is that non-dispersed nanotubes with/without adsorbed MTO formed larger and more abundant agglomerates (Figure 4, panels aA, aB, bE, and bF) than MWCNT-OX (Figure 4, panels aC, and aD) or MWCNT-MTO dispersed in 0.5% BSA (Figure 4, panels bG and bH). The difference was grater at the longer incubation time (144 h). Moreover, cells surrounded the MWCNT-OX or MWCNT-MTO complex almost entirely, and the nanotubes appeared as platforms on which cells could proliferate (Figure 4, panels aB and bF). On the contrary, MWCNT-OX or MWCNT-MTO suspended in 0.5 % BSA did not show large sized aggregates at 24 h (Figure 4, panels aC and bG, respectively) or 144 h (Figure 4, panels aD and bH, respectively). Similar results were obtained using as a dispersant agent DMSO 0.1% (data not shown). Because of its dispersing properties, stability and biocompatibility, BSA was finally chosen as a dispersant for the cell viability experiments.

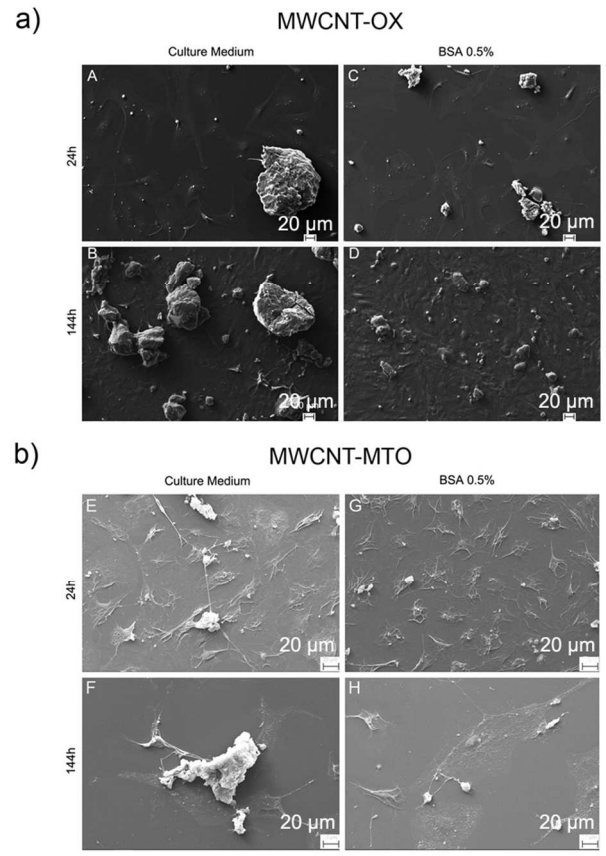

Figure 4. SEM images of MDA 231 cells with MWCNT-OX(Figure 4a) or with MWCNT-MTO (Figure 4b). Images were taken after two incubation times (24 and 144 h) and in two different conditions: without dispersing agent (culture medium) at 24 h (aA and bE) and 144 h (aB and bF), and with BSA 0.5 % as dispersing agent at 24 h (aC and bG) and 144 h (aD and bH), for MWCNT-OX (a) and MWCNT-MTO (b), respectively. The scale bar shown represents 20 µm in all panels.

3.3. MWCNT-OX cytotoxicity

In Figure 5 the cell viability is reported for MDA 231 (Figure 5A) and NIH3T3 cells (Figure 5B) incubated with increasing concentrations (from 0.4 µg/mL to 3 µg/mL) of MWCNT-OX at 24 h, 72 h and 144 h, respectively.

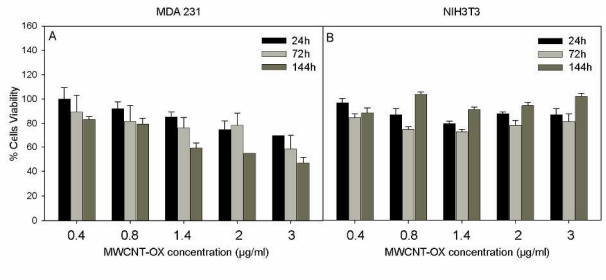

Figure 5. Dose- and time-dependent effect of MWCNT-OX incubated with MDA 231 (A) and NIH3T3 (B) cells. Both types of cell were cultured at a density of 1 x 10^4 cells/well with increasing concentrations (from 0.4 to 3 µg/ml) of MWCNT-OX dispersed in 0.5 % BSA, at three different times (24 h, 72 h and 144 h).

The data are presented as percentage of cell viability in the absence of MWCNT-OX set at 100 %. In general, the viability of both cell types was influenced by the presence of increasing concentrations of MWCNT-OX after different incubation times. Viability values were higher at 24 h even at high concentrations (3 µg/mL) of MWCNT-OX (87 ± 5 % for NIH3T3 and 70 ± 0 % for MDA 231), when compared to 72 h, reaching mortality values of around 30 % for NIH3T3 and 40 % for MDA 231 cells (Figure 5). Interestingly at 144 h, the viability of MDA 231 cells was drastically reduced to 47 ± 4 % using 3 µg/ml when compared with that of NIH3T3 cells treated with the same amount of MWCNT-OX and the same incubation time (102 ± 3%) (Figure 5). For MDA 231, the cell viability trend following treatment with MWCNT-OX was dose- and time-dependent. On the contrary, this dependence was not observed for NIH3T3 cells (Figure 5). In fact, cell viability is always > 70 % for concentration range from 0.4 to 1.4µg/mL and in some case at 144 h viability is higher than 100 %.

The dose of 0.4 µg/mL MWCNT-OX, which showed a very low level of cytotoxicity for both cell types was selected for the apoptosis assay (Figure 6), cell internalization experiments (Figure 7) and for MTO release (Figure 8).

To determine whether MWCNT-OX treatment provoked cell apoptosis, PSVue480^{TM} reagents and propidium iodide (PI) staining were performed at two incubation times, 24 h and 144 h (Figure 6). On the same days as the dye exclusion test, CLSM analysis was performed on untreated cells (negative control), H_2O_2 (positive control), and MWCNT-OX treated cells. As expected, MDA 231 and NIH3T3 cells exhibited markedly green fluorescence after hydrogen peroxide treatment at 24 h (Figure 6A and G) and 144 h (Figure 6D, and J) showing a high level of apoptosis. On the contrary, CLSM analysis at 24 h and 144 h of MDA 231 and NIH3T3, untreated (Figure 6B, E, H, and K) and MWCNT-OX treated (Fig. 6C, F, I, and L),were negative after staining with PSVue480^{TM} reagents, indicating that the MWCNT-OX treatment did not induce apoptosis in either cell types.

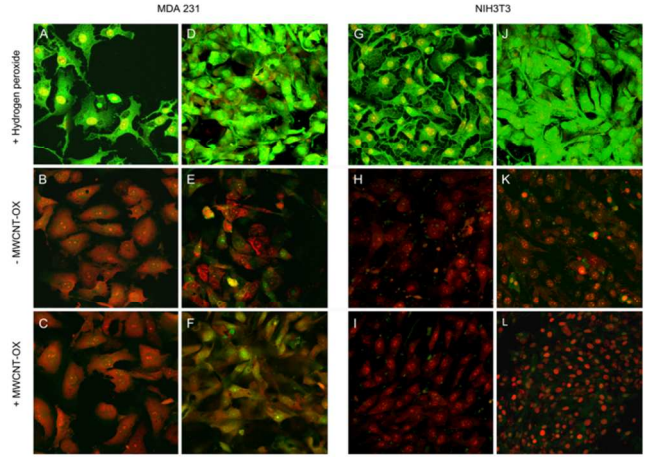

Figure 6. CLSM images of the apoptosis assay. MDA 231 and NIH3T3 cells were cultured for 24 h (panels A, B, C and G, H, I) and 144 h (panels D, E, F and J, K, L) under different conditions

as indicated: positive controls with hydrogen peroxide (A and D; G and J); negative control without MWCNT-OX (B and E; H and K); with MWCNT-OX (C and F; I and L). PSVue480™ reagent was used to evaluate apoptotic cells in both MDA 231 (panels A, B, C, D, E, F) and NIH3T3 (panels G, H, I, J, K, L) cells, respectively. CLSM images were magnified at 40×.

3.4. MWCNT-OX and MWCNT-MTO cell uptake

MWCNT-OX or MWCNT-MTO internalization by both cell types at a concentration of 0.4 µg/mL in 0.5 % BSA was evaluated by TEM analysis at 3 h, 24 h and 144 h. Interestingly, no MWCNT-OX or MWCNT-MTO complexes were observed after 3 h incubation for either cells type (data not shown).Figure 7 shows TEM images representative of cells cultured with MWCNT-OX (Figure 7a) or MWCNT-MTO complexes (Figure 7b) for 24 hand 144 h. The MWCNT-OX or MWCNT-MTO complexes were observed near the nuclei and cytoplasm of both cell types. MWCNT-OX (Figure 7a) or MWCNT-MTO (Figure 7b) cellular internalization was highly visible at 24 h showing small phagolysosomes containing dispersed carbon nantotubes in both cell types (Figure 7, panels aA, aC, bE and bG).

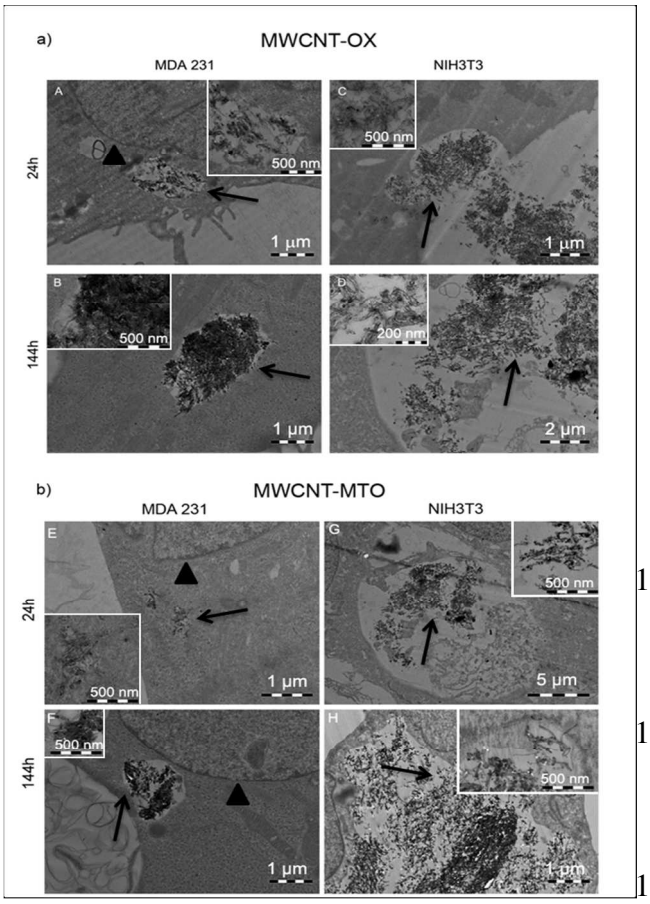

Figure 7. TEM images of the two cell lines cultured with MWCNT-OX (Figure 7a) and with MWCNT-MTO (Figure 7b). MWCNT-OX or MWCNT-MTO (arrows) and cellular nuclei (arrow points) are indicated in the figures. Figure 7a: MDA 231 (A and B) and NIH3T3 (C and D) cells, at 24 h (A and C) and 144 h (B and D). The scale bar shown represents 1 µm (A, B and C), 2 µm (panel D), 500 nm (insert of panels A, B and C) and 200 nm (insert of panel D).Figure 7b: MDA 231 (E and F) and NIH3T3 (G and H) cells, at 24 h (E and G) and 144 h (F and H). The scale bar shown represents 1 µm (panels E, F and H), 5 µm (panel G) and 500 nm (insert of each panels).

On the contrary, at 144 h both MWCNT-OX or MWCNT-MTO detected in the phagolysosomes formed aggregates (Figure 7, panels aB, aD, bF and bH) as observed before BSA dispersion. Apparently, even thought the size of phagolysosomes was greater at 144 h rather than 24 h cultures, nanotubes that entered both cell types did not cause any visible cell damage, as confirmed by the presence of an intact cell membrane and mitochondria. Similar observations were obtained with both cells types incubated with MWCNT-MTO at 144 h if compared to 24 h. Interestingly, at 144 h both MWCNT-OX or MWCNT-MTO seemed to be more packed and assembled in the MDA 231 cells (Figure 7, panels aB and bF, respectively) when compared with those observed in NIH3T3 cells (Figure 7, panels aD and bH, respectively).

3.5.*In vitro* MTO kinetic release

After identification of the non cytotoxic minimal dose for both cell types, the *in vitro* kinetic release of MTO adsorbed on MWCNTs was analysed in the culture medium not containing the cells. The EDC-MWCNT-MTO and DCC-MWCNT-MTO complexes did not release the drug into the cell media (< 5 % release) for any time frame tested (0 h to 144 h).

The release of MTO from MWCNT-MTO electrostatic complexes, loaded with20 mg MTO/g and 160 mg MTO/g is reported in Figure 8.

The time/release relationship is linear till 20 hours reaching then a plateau (t > 24 h, 20-30 % maximum release of the drug loaded) in the absence of cells which could take up the drug, the MTO released is in equilibrium with the one re-adsorbed on the surface. In literature, the release rates are described in terms of power laws giving information on the release mechanism[42,43]. In our case a row fit (data not shown) suggests a Fickian mechanism for the release[44].On the one hand, linear release is highly desirable to maintain the drug concentration in the therapeutic range; on the other hand, slow drug release is important to avoid a MTO overdose, thereby limiting undesired side effects and avoiding tumour lysis syndrome, which is observed when a massive release of the drug onto the neoplastic cells takes place[45].

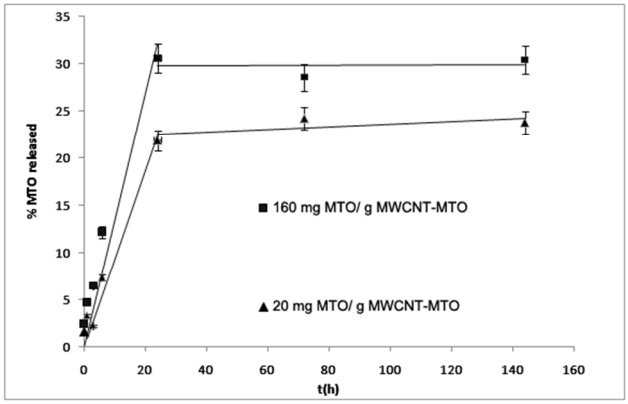

Figure 8. Drug release from MWCNT-MTO (adsorbed). The rate

of release was tested on MWCNT-MTO loaded with 20 mg MTO/g (■) and 160 mg MTO/g MTO (▲).Standard deviations are reported. Lines are only a guide for the eyes.

3.6. MWCNT-MTO and free MTO cytotoxicity efficacy

Cytotoxicity tests were conducted using MWCNT-MTO at a concentration of 0.4 µg/mL (MWCNT-MTO loading 20 mg MTO/g MWCNT-MTO and 160 mg MTO/g MWCNT-MTO were tested; these were compared with a 3.50 ng/mL and 9.92 ng/mL free MTO in solution, as this is the quantity of MTO that these MWCNT-MTO could respectively release); different incubation times (24 h, 72 h and 144 h) were tested with MDA 231 or NIH3T3 cells, comparing MWCNT-MTO effectiveness with MTO in solution at the same doses. Results are presented in Figure 9.

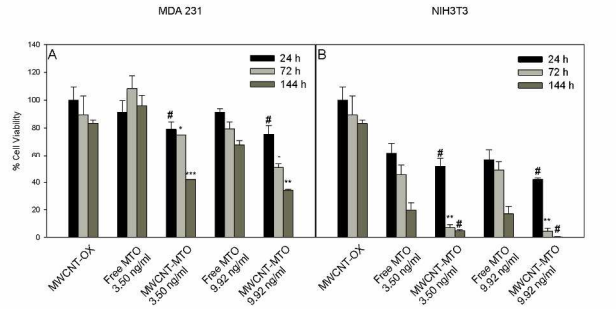

Figure 9. Effect of MTO (free and loaded) on MDA 231 (panel A) and NIH3T3 cells (panel B). Cells were cultured at a density of 1 x 10^4 cells/well at two different concentrations (3.50 and 9.92 ng/ml) of MTO or MWCNT-MTO for three different incubation times: 24 h, 72 h and 144 h. (* $p<0.05$; ** $p<0.005$; *** $p<0.0005$).

It appears that the free drug, at the indicated doses, was more effective on NIH3T3 than on MDA 231 cells and this effect was grater at longer incubation times (144 h). A similar trend was observed for the two MWCNT-MTO drug doses and the indicated incubation times. In particular, after a short incubation the efficacy of MTO free or adsorbed on MDA 231 was not dose-dependent (91 ± 8 % and 91 ± 2 % of cell viability for respectively 3.50 and 9.92 ng/ml concentrations of free drug see panel 9A). On the contrary, on NIH3T3 at 24 h the effect was already evident with a dose of 3.50 ng/mL and did not increased using an higher dose of MTO free or loaded (62 ± 7 % and 56 ± 8 % of cell viability for respectively 3.50 and 9.92 ng/ml concentrations of free drug see panel 9B). At the intermediate incubation time (72 h), the results varied: MDA 231 viability decreased to a greater extent when cells were incubated with MWCNT-MTO in the presence of MTO free in solution at similar concentration (108 ± 9 % and 79 ± 5 % of cell viability for respectively 3.50 and 9.92 ng/ml concentrations of free drug and 75 ± 0 % and 51 ± 3 % of cell viability for respectively 3.50 and 9.92 ng/ml concentrations of drug loaded, see panel 9A). For NIH3T3, cell viability was reduced to 50 % with free drug, but it was significantly reduced up to 90 % with MWCNT-MTO (46 ± 7 % and 49 ± 7 % of cell viability for respectively 3.50 and 9.92 ng/ml concentrations of free drug and 7.14 ± 2 % and 4.60 ± 2 % of cell viability for respectively 3.50 and 9.92 ng/ml concentrations of drug loaded, see panel 9B). At longer incubation times (144 h), the effect of MTO adsorbed was greater on MDA 231 when compared to free MTO (96 ± 7 % and 68 ± 3 % of cell viability for respectively 3.50 and 9.92 ng/ml concentrations of free drug and 42 ± 0 % and 34 ± 1 % of cell viability for respectively 3.50 and 9.92 ng/ml concentrations of drug loaded, see panel 9A). At 144 h, the effect was dramatic on NIH3T3 cells whether incubated with the free drug or adsorbed MTO (20 ± 5 % and 17 ± 5 % of cell viability for respectively 3.50 and 9.92 ng/ml concentrations of free drug and 4.94 ± 1 % and 0.34 ± 1 % of cell viability for respectively 3.50 and 9.92 ng/ml concentrations, of drug loaded, see panel 9B). Regarding MDA 231 cells, the efficacy of MWCNT-MTO greatly increased with time and dose when compared to the addition of free MTO: at 144 h mortality reached values within 60 and 90 % for the lower and the higher concentrations of MTO adsorbed, whereas with free drug it was not significantly altered. In contrast with MDA 231, the time- and dose-dependence was equally evident on NIH3T3 independently of using the free drug or MWCNT-MTO: cell mortality was very pronounced already at 24 h (about 60 %) and increased rapidly to about 100 % at 144 h (see panel 9B).

4.0. Discussion

To overcome limitations associated with the adverse effects of chemotherapeutics drugs, one approach is to develop a nanoformulation to reduce the inherent systemic toxicity of the drugs and to improve their therapeutic effect locally. Despite its promising therapeutic effects, the widespread use of mitoxantrone for the treatment of non-Hodgkin's lymphomas, acute myeloid leukemia, and breast cancer is hindered by potential adverse events. Cardiotoxicity is a major concern; mitoxantrone treatment can result in cardiomyopathy leading to reduced left ventricular ejection fraction and irreversible congestive heart failure[46]. Risk increases with cumulative doses[47] limiting the recommended lifetime dose. Other potential adverse events include myelosuppression, which may lead to anemia, neutropenia or leukopenia, and liver toxicity. MTO exerts antiproliferative activity in advanced breast cancer, acute leukemia, non-Hodgkins lymphoma and chronic myeloid leukemia[48]. Alternative delivery approaches have been evaluated such as the development and characterization of various nanoparticles loaded with mitoxantrone[49-53]. Most of these studies have been performed *in vitro* and none have translated to clinical trial phase II. Recently carbon nanotubes have attracted a widespread interest in nanomedicine as diagnostic or therapeutic tools. In particular, the use of carbon nanotubes to facilitate anticancer drug delivery and improve drug activity seems promising given the capacity of MWCNTs to cross biological barriers[54]. In this *in vitro* study we have investigated for the first time the ability of MTO to interact non covalently with MWCNT-OX at various mass ratios and evaluated their ability to kill human breast cancer cells. Furthermore, we have described for the first time a comparative study on the effect of MWCNT-MTO supramolecolar complexes on NIH3T3 cell survived.

Commercial MWCNTs were purified to eliminate metallic impurities and an oxidation step succeeded in introducing carboxylic acid functionalities on the MWCNT surface (MWCNT-OX) as previously reported[27,28]. To optimize drug delivery system we used MWCNTs with diameters in the range

of 1 – 3 nm for the inner tubes and 2 – 100 nm for the outer tubes. The choice of MWCNTs instead of SWCNTs was justified for a number of reasons. In terms of the structure, it is known that the basic carbon arrangement of SWCNT is different from that of MWCNT[55]. In drug delivery, SWCNTs are known to be more efficient than MWCNTs: they present a one-dimensional structure and an efficient drug-loading capacity due to their ultrahigh surface area[56]. However, drugs conjugated to both CNT types for the delivery of therapeutics in cancer therapy were recently evalueted[15] and it was demonstrated that both SWCNTs and MWCNTs offer analogues available surface area for π-π interactions with the drug, leading to enhanced cell killing efficacy. However, based previous published data and the case of manipulation with the MWCNT, we choose this over the SWCNT. Furthermore, the application of our developed nanosystem may be used for *in situ* application (i.e. during breast cancer surgical procedures) in order to reduce dispersion of metastases through the lymph nodes.

We developed an efficient protocol for MTO binding to MWCNTs by using both covalent (by DCC and EDC) and non-covalent methods. The results in MTO binding capacity showed no significant difference between the two methods as reported before. Although, covalent attachment is recognize as a feasible procedure, it has been suggested that it may cause chemical changes in anticancer drugs, implying that their efficacy could potentially be altered[8]. Consequently, to avoid this possibility, the following experiments were performed with non-covalent attachment of MTO to MWCNT-OX. However, one of the disadvantages of non-covalent bonding is the lack of efficient attachment, potentially resulting in release of the drug before it reaches its site of action[57,58]. For this reason we monitored the MTO release and confirmed that the device is sufficiently stable for 144 h and that the drug is gradually released from the vector. This was also confirmed by the physical and chemical characterizations through TGA analysis, Raman spectra and TEM.

In order to perform the cytotoxicity assays, we first evaluated by SEM analysis the tendency of the non-covalently functionalized MWCNT-OX or MWCNT-MTO to agglomerate and aggregate as a result of weak and strong forces, measuring respectively, van deer Waals forces, electrostatic forces, and sintered bonds. As previously reported[33], the MWCNT-OX or MWCNT-MTO directly dispersed in culture medium tended to form microscopic agglomerates around 100 μm in size. After using 0.5 % BSA as a dispersant agent, the agglomerates were strongly or completely reduced as documented by SEM observation and by the degree of macrodispersion in 0.5 % BSA (data not shown). It has been reported that the dispersion medium can decrease and mask particle toxicity by coating the particles but it is also true that BSA as a biological fluid improve the dispersion and prevents toxic variation due to agglomeration[33]. No significant differences were observed with both MWCNT-OX or MWCNT-MTO dispersed in BSA. Therefore, the choice of using 0.5 % BSA as a dispersant was pertinent and was used for all the subsequent *in vitro* studies.

Regarding MWCNT-OX cytocompatibility, we determined the lowest concentration of MWCNT-OX that triggered a low amount of cytotoxic effects (around 10 - 15 %) in MDA 231 and NIH3T3 cells at different incubation times (Trypan blue dye exclusion assay). Cell viability was not performed with test systems such as the LDH release or MTT assay because interference of MWCNTs with both assays has been observed. Furthermore, the choice of cell type was justified: a well-known human metastatic breast cancer cell line, MDA 231, was used as the experimental model, because it retains the characteristic features of cancer cells such as purity, ease of propagation and genetic manipulation to provide reproducible results[54]. NIH3T3, a non-neoplastic fibroblast cell line was used for comparative analysis with MDA 231 cancer cells. The results were quite interesting: incubation of MWCNT-OX with MDA 231 showed a dose- and time-dependent reduction in cell survival, whereas with NIH3T3 this effect was significantly less showing instead grater cell viability at 144 h. These last data with NIH3T3 contrast those of a previous study performed with human dermal fibroblasts[59] which exhibited MWCNTs dose-dependence cytotoxicity. Regarding the controversial results for MWCNTs cytocompatibility, differences may be attributable to differences in the cell type, in the source and concentrations of MWCNTs used, and the method utilized. In particular, in our study the concentration of MWCNTs used was approximately ten-fold lower, highlighting the importance of MWCNTs dose used for the experiments. In this study, we were able to visualize by TEM the internalization of both MWCNT-OX or MWCNT-MTO into MDA 231 and NIH3T3 cells under standard culture conditions. TEM observation revealed that MWCNT-OX or MWCNT-MTO internalization by NIH3T3 cells is quantitatively more visible at shorter incubation times, whereas at 144 h both types of complexes were more dispersed inside the cell. On the contrary, for MDA 231 cells, the internalization of both MWCNT-OX or MWCNT-MTO was more prominent at longer incubation times showing a more compact quantity of carbon nanotubes when compared with cells cultured for 24 h. Our TEM observations suggest that the cancer cell line is more resistant to the internalization of these nanomaterial systems at 24 h and that they accumulate and condense both MWCNT-OX or MWCNT-MTO at longer incubation times. These observations are confirmed by the previous viability data. Although the specific mechanism of MWCNT-OX or internalization was not examined, our findings suggest that it may occur through either a needle-like action, or endocytosis/phagocytosis[60-63].Furthermore, our data seems to show that the internalization process is independent of the MTO adsorption of MWCNT-OX.

The cytotoxic effect of MTO adsorbed on MWCNT-OX in both MDA 231 and NIH3T3 cells suggested the greater effectiveness of the drug delivery system in comparison with free drug at a similar dose. The trend was similar for dose and incubation times for both cell types but unexpectedly the effect was even more pronounced in NIH3T3 cells. The mitoxantrone mechanism of action should be kept in mind: it is a DNA-reactive agent that intercalates into deoxyribonucleic acid (DNA) through hydrogen bonding, causing crosslinks and strand breaks[22]. Mitoxantrone also interferes with ribonucleic acid (RNA) and is a potent inhibitor of topoisomerase II, an enzyme responsible for uncoiling and repairing damaged DNA. Furthermore, it has a cytocidal effect on both proliferating and non-proliferating cultured human cells, suggesting a lack of cell cycle phase

specificity. On this basis, we may argue that the greater cytotoxic effect seen in NIH3T3, representing a non-neoplastic cell line, is due to the combination of the MTWCNT-OX with the MTO and not only to the MWCNT. Nevertheless, it should be pointed out that this effect is already higher simply with the free drug when compared with the same dose and incubation times in MDA 231 cells. The entry of MWCNT-MTO as previously shown by TEM may promote better delivery of the drug inside the cells. But the prepared drug delivery system did not distinguish cancer from non-neoplastic cells. This aspect should be kept in mind when developing for possible medical applications.

5.0. Conclusions

In summary, we present for the first time data on the adsorption of MTO to functionalized MWCNTs and a comparative analysis of its *in vitro* suitability as a drug delivery system against cancer and non-neoplastic cells. In our study, we determined the dose of MWCNT-OX which was not cytotoxic and did not promote apoptosis in either cell type. We further documented their cell internalization after 24 h by TEM analysis. The drug non covalently adsorbed on MWCNTs was evaluated for release and its effect on both cell types showed its efficacy in killing cells. Although this drug delivery system may be interesting, further *in vitro* and *in vivo* studies need to be performed before validation in *in situ* local applications.

6.0 Acknowledgments

This study was supported by "Project SAL-45" financed by the Regione Lombardia (2010) and by a project financed by the Fondazione Alma Mater Ticinensis (2010). L.V. also thanks the Italian Ministero dell'Istruzione, dell'Università e della Ricerca (grant: PRIN 2011, NanoMed n° 2010 FPTBSH_009).The authors would like to acknowledge financial support from the Health Italian Ministry, RICERCA FINALIZZATA 2009, entitled "Integrated Approach To Evaluate Biological Effects On Lung, Cardiovascular System And Skin Of Occupational Exposure To NaNomaterials (NanO I-LuCaS), n° RF-2009-1472550.

We are grateful to D. Picenoni (Politecnico di Milano, Milano, Italy), Dr P. Vaghi and Dr V. Necchi (Centro Grandi Strumenti, University of Pavia, Pavia, Italy) for their technical assistance in the SEM, CLSM and TEM studies, respectively. A special thanks to Laurene Kelly for correcting the English.

7.0 Notes and references

[1] Dept. of Chemistry, University of Pavia, Italy
[2]Dept. of Molecular Medicine, Center for Tissue Engineering (C.I.T.), INSTM UdR of Pavia, University of Pavia, Italy
[3]Dept. of Public Health, Experimental and Forensic Medicine, University of Pavia, Italy
[4]Dept. of Occupational Medicine, Ergonomy and Disability, Laboratory of Nanotechnology, Salvatore Maugeri Foundation, IRCCS, Pavia, Italy

1 R. A. Siegel, M. J. Rathbone, *Fundamentals and Applications of Controlled Release Drug Delivery*, 2012, 19-43.
2 G. Hermerén, *NanoEthics* **2007**, *1(3)*, 223-237.
3 A. Bianco, K. Kostarelos, M. Prato, *Current Opinion in Chemical Biology* **2005**, *9*, 674–679.
4 M. Endo, M. Strano, P. Ajayan, *Topics in Applied Physics* 2008, **111**, 13–62.
5 T. Murakami, K. Ajima, J. Miyawaki,M. Yudasaka, S. Iijima, K. Shiba, *Molecular Pharmaceutics* **2004**, *1(6)*, 399–405.
6 S. J. Son, X. Bai, S.B. Lee, *Drug Discovery Today* **2007**, *12(15/16)*, 650–656.
7 X. Wang, J. Ren, X. Qu, *ChemMedChem* **2008**, *3(6)*, 940–945.
8 Z. Liu, X. Sun, N. Nakayama-Ratchford, H. Dai, *ACS Nano* **2007**, *1(1)*, 50–56.
9 M. R. McDevitt, D. Chattopadhyay, B. J. Kappel, J. Singh Jaggi, S. R. Schiffman, C. Antczak, J. T. Njardarson, R. Brentjens, D. A. Scheinberg, *The Journal of Nuclear Medicine* **2007**, *48(7)*, 1180–1189.
10 N. Venkatesan, J. Yoshimitsu, Y. Ito, N. Shibata, K. Takada, *Biomaterials* **2005**, *26(34)*, 7154–7163.
11 D. Van Berlo, M. J. D. Clift, C. Albrecht, R. P. F. Schins, *Swiss Medical Weekly* **2012**, *142*, 1-16.
12 Y. Zhang, B. Wang, X. Meng, G. Sun, C. Gao, *Healing Annals of Biomedical Engineering* **2011**, *39*, 414-426.
13 S. Iijima, *Physica B* **2002**, *323*, 1–5.
14 S. Y. Madani, N. Naderi, O. Dissanayake, A. Tan, A. M. Seifalian, *International Journal of Nanomedicine* **2011**, *6*, 2963–2979.
15 H. Ali-Boucetta, K. T. Al-Jamal, D. McCarthy, M. Prato, A. Bianco, K. Kostarelos, *Chemical Communications* **2008**, 459-461.
16 Z. Sobhani, R. Dinarvand, F. Atyabi, M. Ghahremani, M. Adeli, *International Journal of Nanomedicine* **2011**, *6*, 705-719.
17 C. Samorì, H. Ali-Boucetta, R. Sainz, C. Guo, F. M. Toma, C. Fabbro, T. Da Ros, M. Prato, K. Kostarelos, A. Bianco, *Chemical Communications* **2010**, *46*, 1494-1946.
18 W. Wu, R. Li, X. Bian, Z. Zhu, D. Ding, X. Li, Z. Jia, X. Jiang, Y. Hu, *ACS Nano* **2009**, *3(9)*, 2740-2750.
19 D. Ravelli S. Montanaro, C. Tomasi, P. Galinetto, E. Quartarone, D. Merli, P. Mustarelli, M. Fagnoni, *ChemPlusChem* **2012**, *77(3)*, 210-216.
20 L. Wu, C. Man, H. Wang, X. Lu, Q. Ma, Y. Cai, W. Ma, *Pharmaceutical Research* **2013**, *30*, 412-423.
21 D. Ravelli, D. Merli, E. Quartarone, A. Profumo, P. Mustarelli, M. Fagnoni, *RSC Advances* **2013**, *3*, 13569-13582.
22 F. E. Durr, R. E. Wallace, R. V. Citarella, *Cancer Treatment Reviews* **1983**, *10(Suppl B)*, 3–11.
23 I. E. Smith, *Cancer Treatment Reviews* **1983**, *10*, 103–115.
24 F. Martinelli Boneschi, L. Vacchi, M. Rovaris, R. Capra, G. Comi, *The Cochrane Collaboration* **2013**, *5*, 1-29.
25 W. A. Sibley, *A guide to treatments. 4th edition*.1996.
26 D. Merli, M. Ugonino, A. Profumo, M. Fagnoni, E. Quartarone, P. Mustarelli, L. Visai, M.S. Grandi, P. Galinetto, P. Canton, *Journal of Nanoscience and Nanotechnology* **2011**, *11(4)*, 3100-3106.
27 A. Profumo, M. Fagnoni, D. Merli, E. Quartarone, S. Protti, D. Dondi, A. Albini, *Analytical Chemistry* **2006**, *78(12)*, 4194-4199.
28 D. Merli, A. Profumo, D. Dondi, A. Albini, *ChemPhysChem* **2009**, *10(7)*, 1090-1096.
29 G. C. Jensen, X. Yu, J. D. Gong, B. Munge, A. Bhirde, S. N. Kim, F. Papadimitrakopoulos, J. F. Rusling, *Journal of Nanoscience and Nanotechnology* **2009**, *9(1)*, 249-255.
30 Y. S. Rho, G. Kim, W. J. Kim, S. Park, D. J. Yoo, H. S. Kang, S. R. Chung, *Bulletin of the Korean Chemical Society* **2001**, *22(6)*, 587-592.
31 Y-M Peng, D. Omberg, D. S. Alberts, *Journal of Chromatografy B* **1982**, *233(1)*, 235-242.
32 R. Cailleau, R. Young, M. Olive, W. J. Reeves, *Journal of the National Cancer Institute* **1974**, *53*, 661– 674.
33 J. S. Kim, K. S. Song, J. H. Lee, I. J. Yu, *Archives of Toxicology* **2011**, *85(12)*, 1499-1508.
34 E. Saino, V. Maliardi, E. Quartarone, L. Fassina, L. Benedetti, M. G. Cusella De Angelis, P. Mustarelli, A. Facchini, L. Visai, *Tissue Engineering* **2010**, *16(3)*, 995-1008.
35 W. Strober, *Current Protocols in Immunology* 1997.

36 M. Van Engeland, L. J. W. Nieland, F. C. S. Ramaekers, B. Schutte, C. P. M. Reutelingsperger, *Cytometry* **1998**, *31(1)*, 1-9.

37 J. Kersigo, A. D'Angelo, B. D. Gray, G. A. Soukup, B. Fritzsch, *Genesis* **2011**, *49*, 326-341.

38 M. A. Hayat, *Principles and Techniques of Electron Microscopy—Biological Applications*, 2000.

39 E. S. Gil, L. Wu, L. Xu, T. L. Lowe, *Biomacromolecules* **2012**, *13(11)*, 3533-3541.

40 M. S. Dresselhaus, R. Saito, A. Jorio, *Physics Reports* **2005**, *409(2)*, 47-99.

41 D. Q. Yang, J. F. Rochette, E. Sacher, *Journal of Physical Chemistry B* **2005**, *109(16)*, 7788-7794.

42 L. Wu, C. S. Brazel, *International Journal of Pharmaceutics* **2008**, *349*, 1-10.

43 L. Wu, C. S. Brazel, *International Journal of Pharmaceutics* **2008**, *349*, 144-151.

44 X. Huang, C. S. Brazel, *Journal of Controlled Release* **2001**, *73*, 121-136

45 S. C. Howard, D. P. Jones, C. H. Pui, *The New England Journal of Medicine* **2011**, *364*, 1844-1854.

46 V. B. Pai, M. C. Nahata, *Drug Safety* **2000**, *22*, 263–302.

47 F. J. Mather, R. M. Simon, G. M. Clark, D. D. Von Hoff, *Cancer Treatment Reports* **1987**, *71*, 609–613.

48 B. S. Parker, T. Buley, B. J. Evison, S.M. Cutts, G. M. Neumann, M. N. Iskander, D. R. Phillips, *Journal of Biological Chemistry* **2004**, *279(18)*, 18814-18823.

49 K. J. Lee, J. H. An, J. R. Chun, K. H. Chung, W. Y. Park, J. S. Shin, D. H. Kim, Y. Y. Bahk, *Journal of Biomedical Nanotechnology* **2013**, *9(6)*, 1071-1075.

50 A. Tzur-Balter, A. Gilert, N.Massad-Ivanir, E. Segal, *Acta Biomaterialia* **2013**, *9(4)*, 6208-6217.

51 S. Grund, T. Doussineau, D. Fischer, G. J. Mohr, *Journal of Colloid and Interface Science* **2012**, *365(1)*, 33-40.

52 L. K. Zhang, S. X. Hou, J. Q. Zhang, W. J. Hu, C. Y. Wang, *Archives of Pharmacal Research* **2010**, *33(8)*, 1193-1198.

53 H. Chen, W. Yang, H. Chen, L. Liu, F. Gao, X. Yang, Q. Jiang, Q. Zhang, Y. Wang, *Colloids and Surfaces B: Biointerfaces* **2009**, *73(2)*, 212-218.

54 K. Kostarelos, L. Lacerda, G. Pastorin, W. Wu, S. Wieckwski, J. Luangsivilay, S. Godefroy, D. Pantarotto, J. P. Briand, S. Muller, M. Prato,A. Bianco, *Nature Nanotechnology* **2007**, *2*, 108-113.

55 D. Danailov, P. Keblinski, S. Nayak, P. M. Ajayan, *Journal of Nanoscience and Nanotechnolgy* **2002**, *2*, 503–507.

56 R. P. Feazell, N. Nakayama-Ratchford, H. Dai, S. J. Lippard, *Journal of American Chemical Society* **2007**, *129*, 8438–8439.

57 N. W. Shi Kam, T. C. Jessop, P. A. Wender, H. Dai, *Journal of American Chemical Society* **2004**, *126*, 6850–6851.

58 M. M. Gottesman, T. Fojo, S. E. Bates, *Nature Review Cancer* **2002**, *2*, 48–58.

59 P. Kesharwani, R. Ghanghoria, N. K. Jain, *Drug Discovery Today* **2012**, *17(17/18)*, 1023-1030.

60 A. Patlolla, B. Patlolla, P. Tchounwou, *Molecular and Cellular Biochemistry* **2010**, *338(1-2)*, 225-232.

61 D. Pantarotto, R. Singh, D. McCarthy, M. Erhardt, J. P. Briand, M. Prato, K. Kostarelos, A. Bianco, *Angewandte Chemie International Edition in English* **2004**, *43(39)*, 5242–5246.

62 A. Fraczek-Szczypta, E. Menaszek, T. B. Syeda, A. Misra, M. Alavijeh, J. Adu, S. Blazewicz, *Journal of Nanoparticle Research* **2012**, *14*, 1181-1195.

63 H. Haniu, N. Saito, Y. Matsuda, T. Tsukahara, K. Maruyama, Y. Usui, K. Aoki, S. Takanashi, S. Kobayashi, H. Nomura, M. Okamoto, M. Shimizu, H. Kato, *Toxicology in Vitro* **2013**, *27*, 1679–1685.